Neurobiology of Aging 74 (2019) 38–45

Contents lists available at ScienceDirect

Neurobiology of Aging

journal homepage: www.elsevier.com/locate/neuaging

Cortical atrophy pattern–based subtyping predicts prognosis of amnestic MCI: an individual-level analysis

Hee Jin Kim [a,b], Jong-Yun Park [c], Sang Won Seo [a,b,d], Young Hee Jung [a,b], Yeshin Kim [a,b,e], Hyemin Jang [a,b], Sung Tae Kim [f], Joon-Kyung Seong [c,**,1], Duk L. Na [a,b,g,*,1]

[a] Department of Neurology, Samsung Medical Center, Sungkyunkwan University School of Medicine, Seoul, Republic of Korea
[b] Neuroscience Center, Samsung Medical Center, Seoul, Republic of Korea
[c] School of Biomedical Engineering, Korea University, Seoul, Republic of Korea
[d] Department of Clinical Research Design & Evaluation, SAIHST, Sungkyunkwan University, Seoul, Republic of Korea
[e] Department of Neurology, Kangwon National University Hospital, Kangwon National University College of Medicine, Chuncheon, Republic of Korea
[f] Department of Radiology, Samsung Medical Center, Sungkyunkwan University School of Medicine, Seoul, Republic of Korea
[g] Department of Health Sciences and Technology, SAIHST, Sungkyunkwan University, Seoul, Republic of Korea

ARTICLE INFO

Article history:
Received 10 April 2018
Received in revised form 19 September 2018
Accepted 5 October 2018
Available online 12 October 2018

Keywords:
Mild cognitive impairment
Alzheimer's disease
Cortical atrophy pattern
Classifier

ABSTRACT

We categorized patients with amnestic mild cognitive impairment (aMCI) based on cortical atrophy patterns and evaluated whether the prognosis differed across the subtypes. Furthermore, we developed a classifier that learns the cortical atrophy pattern and predicts subtypes at an individual level. A total of 662 patients with aMCI were clustered into 3 subtypes based on cortical atrophy patterns. Of these, 467 patients were followed up for more than 12 months, and the median follow-up duration was 43 months. To predict individual-level subtype, we used a machine learning–based classifier with a 10-fold cross-validation scheme. Patients with aMCI were clustered into 3 subtypes: medial temporal atrophy, minimal atrophy (Min), and parietotemporal atrophy (PT) subtypes. The PT subtype had higher prevalence of APOE ε4 carriers, amyloid PET positivity, and greater risk of dementia conversion than the Min subtype. The accuracy for binary classification was 89.3% (MT vs. Rest), 92.6% (PT vs. Rest), and 86.6% (Min vs. Rest). When we used ensemble model of 3 binary classifiers, the accuracy for predicting the aMCI subtype at an individual level was 89.6%. Patients with aMCI with the PT subtype were more likely to have underlying Alzheimer's disease pathology and showed the worst prognosis. Our classifier may be useful for predicting the prognosis of individual aMCI patients.

1. Introduction

Amnestic mild cognitive impairment (aMCI), a transitional state between normal aging and Alzheimer's disease (AD) dementia (Petersen, 2004), is known to consist of a heterogeneous group of patients (Knopman et al., 2015; McGuinness et al., 2015; Nettiksimmons et al., 2014; Ota et al., 2016; Pusswald et al., 2013). Longitudinal data show that, among patients with aMCI, some convert to AD dementia, whereas others remain in the MCI stage or even revert to normal cognition, suggesting that various etiologies underlie cognitive impairment (Knopman et al., 2015; Vos et al., 2015). In clinical practice, early intervention is needed in individuals who are likely to develop neurodegenerative processes, but timely diagnosis is challenging. Although positron emission tomography (PET) and cerebrospinal fluid (CSF) analyses enable the detection of AD biomarkers (amyloid or tau) (Shim and Morris, 2011), these methods are not yet widely available due to their high cost and invasiveness.

Patterns of cortical atrophy, which precedes cognitive impairment, reflect the underlying pathology and can be used as a reliable biomarker to predict patient prognosis. AD-like cortical atrophy in aMCI can be a sign of underlying AD processes (Dong et al., 2016b; Zhang et al., 2012). However, only a few studies have examined anatomical subtypes of aMCI and their clinical implications (Dong et al., 2016b; Nettiksimmons et al., 2014). Using Alzheimer's Disease Neuroimaging Initiative (ADNI) data, Dong et al. classified patients with aMCI and AD dementia into 4 anatomical subtypes

* Corresponding author at: Department of Neurology, Sungkyunkwan University School of Medicine, Samsung Medical Center, 50 Ilwon-dong, Gangnam-gu, Seoul 135-710, Republic of Korea. Tel: +82-2-3410-3591/-3599, fax: +82-2-3410-0052.
** Corresponding author at: School of Biomedical Engineering, Korea University, Seoul, Republic of Korea. Tel./fax: +82-2-3290-5660.
E-mail addresses: jkseong@korea.ac.kr (J.-K. Seong), dukna@naver.com (D.L. Na).
[1] These authors contributed equally to this work.

0197-4580/$ – see front matter © 2018 Elsevier Inc. All rights reserved.
https://doi.org/10.1016/j.neurobiolaging.2018.10.010

and found that each subtype had distinct clinical features (Dong et al., 2016b). Nettiksimmons et al. also used ADNI data and identified 4 clusters of aMCI patients based on brain structural volume and CSF AD biomarkers (Nettiksimmons et al., 2014). These previous studies performed group analysis and thus have limited value to individual patients because their findings cannot be directly translated to clinical practice.

Herein, we clustered patients with aMCI based on similarities in cortical atrophy patterns. We used the graph-theoretical clustering method (Louvain method), which is robust against sampling bias (Park et al., 2017). We first compared clinical phenotypes between the anatomical subtypes and identified subtypes that have poor prognosis. More importantly, we proposed an individual subject classification method that classifies patients with aMCI using cortical atrophy patterns.

2. Materials and methods

2.1. Participants

We consecutively collected data from 740 patients with aMCI from the Memory Clinic at Samsung Medical Center from July 2007 to December 2012 who underwent detailed neuropsychological testing and brain magnetic resonance imaging (MRI) including 3-dimensional T1 images. All patients were selected based on the following inclusion and exclusion criteria and were >45 years old. The patients met the Petersen's clinical criteria for MCI (Petersen et al., 1999) with the following modifications: (1) subjective memory problems reported by the patient or caregiver, (2) normal activities of daily living (ADL) as judged by an interview with a clinician and the Seoul–Instrumental ADL test (with a score <8) (Ku et al., 2004), (3) objective memory decline below the 16th percentile determined by neuropsychological tests, and (4) no dementia. Exclusion criteria included history of traumatic brain injury, cortical stroke, seizure, brain surgery, and current systemic medical disease that could affect cognition and severe white matter hyperintensities (WMHs) defined as deep WMH ≥25 mm and periventricular WMH ≥10 mm. We also excluded patients who met the Diagnostic and Statistical Manual of Mental Disorders (fourth edition) criteria for psychotic or mood disorders, such as schizophrenia or major depressive disorder (American Psychiatric Association, 2000).

Of the 740 patients who met the aforementioned criteria, 78 were excluded because of segmentation errors during cortical thickness analysis. Therefore, the final sample consisted of 662 patients with aMCI.

320 normal controls (NCs) were selected from individuals who visited the Health Promotion Center of the Samsung Medical Center from September 2008 to December 2012. Inclusion criteria for NCs were as follows: (1) no complaint of subjective memory problems; (2) normal cognitive function, defined by a Mini–Mental State Examination (MMSE) score above the 16th percentile for age- and education-matched norms; (3) no history of neurologic or psychiatric disorders; and (4) no structural abnormalities on brain MRI.

This study was approved by the Institutional Review Board of the Samsung Medical Center.

2.2. Neuropsychological tests

All patients with aMCI underwent neuropsychological tests using a standardized neuropsychological battery called the Seoul Neuropsychological Screening Battery (Ahn et al., 2010; Kang and Na, 2003), the details of which are described in Appendix e-1.

2.3. Amyloid PET acquisition and analysis

We used 18F-florbetaben PET (48 patients) or 11C-Pittsburgh compound B PET (36 patients) to detect amyloid in the brain. We defined florbetaben PET as positive when visual assessment scored 2 or 3 on the brain Aβ plaque load scoring system (Barthel et al., 2011). We defined Pittsburgh compound B PET as positive when the global uptake ratio (using cerebellar gray matter as the reference region) was more than 2 standard deviations from the mean of the normal controls (standardized uptake value ratio ≥1.5) (Lee et al., 2011).

2.4. Vascular risk factors and APOE genotyping

Presence or absence of vascular risk factors such as diabetes, hypertension, and hyperlipidemia was defined by self-report or caregiver's report.

Genomic DNA was extracted from peripheral blood leukocytes using the Wizard Genomic DNA Purification kit following the manufacturer's instructions (Promega, Madison, WI). Two single-nucleotide polymorphisms (SNPs; rs429358 for codon 112 and rs7412 for codon 158) in the APOE gene were genotyped using TaqMan SNP Genotyping Assays (Applied Biosystems, Foster City, CA) on a 7500 Fast Real-Time PCR System (Applied Biosystems) according to the manufacturer's instructions.

2.5. Longitudinal follow-up of patients with aMCI

Of the 662 patients with aMCI, 467 (70.5%) were followed up for more than 12 months. The median follow-up duration was 43 months. The point of dementia conversion was determined by neurologists based on clinical interviews and neuropsychological tests including the instrumental ADL scale. For patients who did not undergo detailed neuropsychological tests (n = 78), neurologists determined dementia conversion based on clinical interviews and the Geriatric Deterioration Scale (Choi et al., 2002).

2.6. MRI acquisition and cortical atrophy pattern–based cluster analysis

An Achieva 3.0-Tesla MRI scanner (Philips, Best, The Netherlands) was used to acquire 3-dimensional T1 turbo field echo MRI data from all participants using the following imaging parameters: sagittal slice thickness, 1.0 mm; over contiguous slices with 50% overlap; no gap; repetition time, 9.9 ms; echo time, 4.6 ms; flip angle, 8°; and matrix size of 240 × 240 pixels reconstructed to 480 × 480 over a field of view of 240 mm. We extracted surfaces of gray and white matter from T1-weighted images using FreeSurfer v5.1.0. (Dale et al., 1999; Dale and Sereno, 1993). We manually checked the quality of the extracted cortical surfaces and corrected them if necessary. The surface meshes were then resampled using 40,962 vertices for each hemisphere. We also used the Laplace-Beltrami operator for diffusion smoothing of cortical thickness data with our in-house software, as in our previous studies (Cho et al., 2012; Qiu et al., 2006).

We adopted our previous clustering method proposed for subtyping patients with very mild AD (Park et al., 2017). This subtyping method creates clusters based on the similarity of cortical atrophy patterns with a graph-theoretical technique. First, we estimated the cortical atrophy patterns of patients with aMCI using the cortical thickness data of the NCs. Specifically, the z-score at each vertex of the cortical surface was calculated from the distribution of cortical thickness in the NC group: $z_i^{aMCI_j} = (c_i^{aMCI_j} - \mu_i^{NC})/\sigma_i^{NC}$, where $z_i^{aMCI_j}$ is the z-score of the i-th vertex of the j-th aMCI patient; i = 1,2, …, 81,924, $c_i^{aMCI_j}$ is the cortical thickness value of the j-th aMCI patient

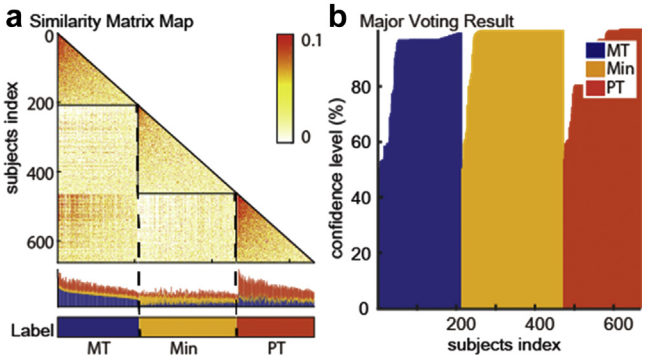

Fig. 1. (A) The similarity matrix map shows the correlation between the whole paired samples. We reordered and drew borders among the subtypes. (B) The major voting result of the subtyping method shows high consistency (92.39%). Subtypes are indicated by color. MT, medial temporal atrophy; Min, minimal atrophy; PT, parieto-temporal atrophy. (For interpretation of the references to color in this figure legend, the reader is referred to the Web version of this article.)

at the i-th vertex; and μ_i^{NC} and σ_i^{NC} are the mean and standard deviation of cortical thickness at the i-th vertex of the NC group, respectively. We then constructed a similarity matrix based on the correlation coefficients for cortical atrophy patterns between any pair of aMCI patients. Finally, we extracted clusters from the similarity matrix by exploiting the Louvain method (Fig. 1). The Louvain method determined the modular organization by maximizing the modularity value Q with denser intramodular connections and sparser intermodular connections. Although the Louvain method is accurate and efficient for large networks, the clustering results vary slightly when analyzed multiple times because the Louvain method finds clusters with a greedy optimization method. We resolved this problem by using a major-voting scheme. Each subject was labeled by the clustering result, which is the most frequently chosen in N repetition results. In addition, the Louvain method is able to manage the number of clusters by controlling the resolution parameter, γ. Similar to our previous study (Murray et al., 2011; Park et al., 2017), we controlled this parameter ($\gamma = 0.9$) and repeated the subtyping procedure 1000 times for the major-voting scheme.

2.7. Optimal number of clusters

It is widely accepted that intracluster distance and intercluster distance are important measures of the quality of a specific clustering. The intracluster distance decreases as homogeneity within clusters increases, whereas the intercluster distance increases as homogeneity between different clusters decreases. A good cluster should minimize intracluster distance and also maximize intercluster distance at the same time. The gamma value in Lurvain's method controls the relative weight for intracluster and intercluster variance to determine the clusters. We performed cluster analysis using a range of gamma values (from 0.7 to 1.0) and examined the clinical implications of the resulting clusters. Because conversion to AD dementia is the most important clinical implication in our problem setting, we used whether the patient converted to AD dementia as a metric for measuring intercluster/intracluster distance. We selected 3 clusters as the optimal clustering number as it had the largest ratio of the intercluster/intracluster distance (Table e-1).

2.8. Reproducibility analysis

We analyzed the reproducibility of the proposed clustering method, which captures how a method provides consistent results. We measured the fraction of consistently assigned subjects to each subtype on average. Our data set was divided into 10 subsets randomly, and we repeatedly performed our method 10 times excluding 1 subset in turn. Next, we computed the average fraction over 10 runs. The subtype label was considered to be reproducible if the subtype label rendered from each subset matched the subtype identified using all of the subjects. We further compared our method (the Louvain method with correlation) with the hierarchical clustering-based method (Noh et al., 2014) and performed the same experiment using the two different methods. For hierarchical clustering, we followed the method suggested by Noh et al. (Noh et al., 2014). The only difference was that we used our estimated cortical atrophy instead of raw cortical thickness for fair comparison. We also performed the experiment using 2 different similarity metrics: the correlation coefficient and Euclidean distance for investigating the effects of the correlation coefficients as a similarity measure.

2.9. Individual subject analysis

To predict individual-level subtype, we used a machine learning–based classification algorithm. Because we have 3 subtypes to predict at an individual level, we developed an ensemble model of 3 binary classifications. Specifically, each binary classifier was constructed for discrimination of each subtype versus the other subtypes. Then, the individual subject's subtype was predicted by combining the results of 3 binary classifications. Our binary classification is based on principal component analysis (PCA) and linear discriminant analysis (LDA) with nested cross-validation (Groth et al., 2013; Liu and Wechsler, 2000; Yu and Yang, 2001). PCA is a statistical dimension reduction method achieved by computing principal components that have the largest variance in the projection of data distribution by linear transformation. LDA finds the axis where the discrepancy within the class is maximized while the variance among the class is minimized. LDA is a commonly used linear classifier for binary classification problems.

In this study, we used nested cross-validation for a performance validation scheme and hyperparameter tuning by dividing the data set with 10% random removal. We further divided the training set into 10 subsets, one for a validation set and the rest for training a classification model. Nested cross-validation consisted of 2 loop procedures: an inner loop and outer loop. First, an inner loop is used for finding the best hyperparameters and training candidate binary classifier models. We constructed 10 candidate binary classifiers from the inner loop iteration and one classifier using the whole train set with the best hyperparameters. We finally determinedan individual subtype label using a major-voting scheme with all 33 classifiers (11 candidate classifiers for each of three subtypes). Second, an outer loop was used for evaluating our subtype prediction model with the unseen test set. During the outer loop, we repeated de novo group-level subtyping using only the training data set. We used the nested cross-validation scheme to avoid so-called "circular performance evaluation" in the subtype prediction. That is, the ground truth label for each test subject was determined based on the whole data set in the outer loop, whereas that of the training data set was derived only from the training data set in the inner loop without seeing the test data set.

2.10. Statistical analyses

To evaluate whether age, gender, education level, and vascular risk factors differed across the anatomical subtypes, we performed analysis of variance or χ^2 test followed by Bonferroni's post hoc analysis to compare groups.

To assess whether dementia risk differed across anatomical subtypes, we applied Cox's proportional hazards model after controlling for age and education level.

We used MATLAB (Version 2014b, MathWorks, Natick, MA, USA) for MRI preprocessing and subtyping (http://bia.korea.ac.kr/software/AD_subtyping/). The SurfStat toolbox was used to visualize the cortical atrophy pattern (http://www.math.mcgill.ca/keith/surfstat).

3. Results

3.1. Anatomical subtypes of aMCI

Patients were clustered into 3 subtypes (Fig. 1A). When we repeated the subtyping procedure 1000 times for the major-voting scheme, the labels were identified with a high consistency of 92.9% (Fig. 1B). We called the first subtype the medial temporal atrophy (MT) subtype (n = 208, 31.4%) because atrophy was mainly localized to bilateral medial temporal areas, especially in the parahippocampal, uncus, and fusiform gyri, compared with the NCs. The second type was the minimal atrophy (Min) subtype (n = 258, 39.0%) in which patients did not show significant cortical thinning compared with NCs. The third type was the parietotemporal atrophy (PT) subtype (n = 196, 29.6%), which showed atrophy predominantly located in the parietal areas (superior and inferior parietal lobules and precuneus) and temporal areas (superior, middle, and inferior temporal gyri) compared with NCs (Fig. 2).

3.2. Baseline characteristics of anatomical subtypes of aMCI

There were no differences in age, gender, or education level across the 3 subtypes. However, compared with patients with the Min subtype, patients with the PT subtype were more likely to be APOE ε4 carriers ($p < 0.001$). Furthermore, patients with the PT subtype were more often positive for amyloid PET, with an amyloid PET positivity of 72.4% as opposed to 42.4% in the Min subtype ($p = 0.017$) (Table 1). Baseline cognitive function did not differ across the 3 subtypes (Table e-2).

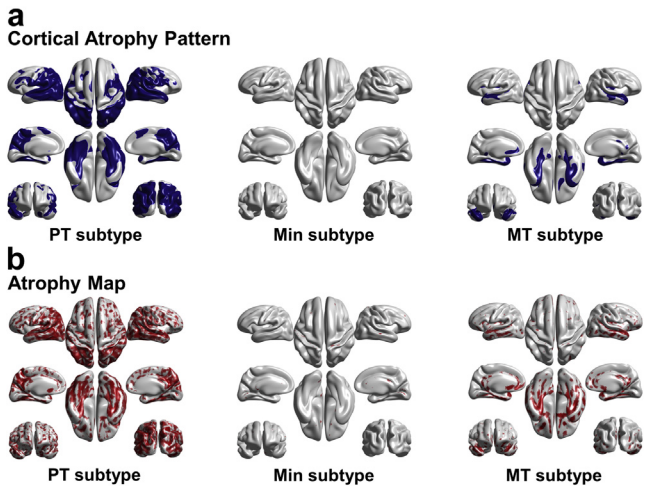

Fig. 2. The 3 anatomical subtypes of amnestic mild cognitive impairment. (A) The colored region shows group comparison results of cortical thickness between each subtype and normal controls, which were corrected using random field theory ($p < 0.001$). (B) The atrophy map shows the median of cortical atrophy (z-score) in each subtype. MT, medial temporal atrophy; Min, minimal atrophy; PT, parietotemporal atrophy. (For interpretation of the references to color in this figure legend, the reader is referred to the Web version of this article.)

3.3. Dementia conversion

We further analyzed 467/662 (70.5%) patients with aMCI who were followed up for more than 12 months. Disease duration and follow-up duration did not differ across the 3 subtypes (Table 1). Among 467 patients with aMCI, 171 (36.7%) patients developed dementia and 66 (14.1%) patients reverted to normal cognition within median follow-up of 43 months. Of 171 patients who developed dementia, 162 patients developed AD dementia and 9 patients developed non-AD dementia, which includes 3 vascular dementia, 1 normal pressure hydrocephalus, 3 progressive supranuclear palsy syndrome, 1 semantic variant primary progressive aphasia, and 1 dementia with Lewy bodies (Table 1). Patients with the PT subtype were at higher risk of dementia conversion than those with the Min subtype, which was significant even after controlling for age and education level (Table 2, Fig. 1).

3.4. Reproducibility in clustering

Our proposed method was highly reproducible and provided consistent results on the mean value for 10 subsets with 10% random removal. Among the various subtyping methods, our method (Louvain method) with correlation coefficients between cortical atrophy patterns had the largest modularity and highest reproducibility (92.94% reproducibility) and outperformed the conventional hierarchical clustering method (81.81% reproducibility) (Table e-3; Fig. 3).

3.5. Prediction of aMCI anatomical subtype at an individual level

We achieved a high classification accuracy in our large aMCI cohort and have summarized the performance in Table e-4. First, we evaluated binary classification performance and achieved accuracy values of 89.3% (MT vs. Rest), 92.6% (PT vs. Rest), and 86.6% (Min vs. Rest). Second, we predicted individual patient subtypes according to the most frequently assigned in a set of candidate binary classifiers. When we used ensemble model of 3 binary classifiers, the overall accuracy for predicting the aMCI subtype at an individual level was 89.6%.

4. Discussion

In this large aMCI cohort, we identified 3 anatomical subtypes of aMCI: the MT subtype (31.4%), Min subtype (39.0%), and PT subtype (29.6%). Among the 3 subtypes, patients with the PT subtype were more likely to have underlying AD pathology and showed the worst prognosis. The overall accuracy for predicting the aMCI subtype at an individual level was 89.6%. These findings therefore emphasize the potential value of clustering patients based on brain atrophy pattern, which could contribute to recruitment of more homogenous patient populations for aMCI clinical trials.

Although a few previous studies investigated anatomical subtypes of MCI, our study has several advantages over the previous 2 studies (Dong et al., 2016b; Nettiksimmons et al., 2014). First, we applied a reliable cortical atrophy pattern–based clustering method. Our clustering method (the Louvain method with correlation) has advantages over conventional methods including its hierarchical clustering, increased robustness against sampling bias, and the ability to distinguish subjects based on cortical atrophy patterns (which represent true anatomical subtype) rather than overall atrophy severity (which is largely influenced by disease stage) (Park et al., 2017). Second, one of the previous studies clustered late aMCI and AD dementia based on voxel-based morphometry and the clustering method named CHIMERA (clustering heterogeneous diseas effect via distribution matching of

Table 1
Demographics of the participants

Characteristics	NCs	Total aMCI	aMCI subtypes			*p*			
			MT subtype	Min subtype	PT subtype				
	N = 320	N = 662	N = 208 (31.4%)	N = 258 (39.0%)	N = 196 (29.6%)	NC vs aMCI	MT vs Min	MT vs PT	Min vs PT
Age, y	70 ± 7.9	70.4 ± 8.4	70.3 ± 8.6	70.0 ± 8.3	71.2 ± 8.3	0.473	1.000	0.859	0.460
Onset age, y		69.1 ± 8.1	68.5 ± 8.2	68.8 ± 8.5	70.1 ± 7.3		1.000	0.273	0.479
Gender (female)	188 (58.8%)	412 (62.2%)	135 (64.9%)	154 (59.7%)	123 (62.8%)	0.294	1.000	1.000	1.000
Education	11.8 ± 5.0	10.5 ± 5.1	10.8 ± 4.9	10.3 ± 5.0	10.4 ± 5.4	<0.001	0.939	1.000	1.000
Vascular risk factors									
Diabetes	79 (24.7%)	217 (32.9%)	74 (35.7%)	82 (31.8%)	61 (31.3%)	0.009	1.000	1.000	1.000
Hypertension	159 (49.7%)	287 (43.4%)	90 (43.3%)	109 (42.2%)	88 (44.9%)	0.062	1.000	1.000	1.000
Hyperlipidemia	102 (31.9%)	194 (29.3%)	71 (34.1%)	69 (26.7%)	54 (27.6%)	0.411	1.000	1.000	1.000
MMSE	27.5 ± 2.5	25.7 ± 3.2	25.8 ± 3.3	25.9 ± 3.0	25.4 ± 3.5	<0.001	1.000	0.817	0.459
GDepS		13.7 ± 7.5	13.50 ± 7.26	14.10 ± 7.37	13.32 ± 7.83		1.000	1.000	0.818
APOE ε4 carrier		198/563 (35.2%)	64/178 (36.0%)	57/211 (27.0%)	77/174 (44.3%)		0.174	0.336	0.001
Amyloid PET positive		48/84 (57.1%)	13/22 (59.1%)	14/33 (42.4%)	21/29 (72.4%)		0.678	0.954	0.049
Mild WMH:Moderate WMH[a]	234:65	478:184	152:56	185:73	141:55	0.047	1.000	1.000	1.000
Cortical thickness, mm	2.35 ± 0.08	2.32 ± 0.10	2.32 ± 0.07	2.38 ± 0.07	2.24 ± 0.10	<0.001	<0.001	<0.001	<0.001
FU duration > 1 y		467 (70.5%)	144 (69.2%)	183 (70.9%)	140 (71.4%)		1.000	1.000	1.000
Reverse to normal cognition		66 (14.1%)	25 (17.4%)	27 (14.8%)	14 (10.0%)		1.000	0.216	0.609
Dementia conversion		171 (36.7%)	48 (33.6%)	58 (31.7%)	65 (46.4%)		1.000	0.081	0.021
AD dementia		159 (34.0%)	45 (31.3%)	54 (29.5%)	63 (42.9%)				
Non-AD dementia		12 (2.6%)	3 (2.1%)	4 (2.2%)	2 (3.6%)				
			[1 NPH and 2 PSPS]	[2 VaD, 1 svPPA, and 1 DLB]	[1 VaD and 1 PSPS]				
Disease duration, months		29.6 ± 23.9	30.8 ± 23.0	27.9 ± 24.0	30.7 ± 24.7		0.842	1.000	0.945
FU duration, months, median (IQR)		43 (30–60)	42 (26–60)	41 (28–59)	44 (32–62)		1.000	1.000	1.000

Key: AD, Alzheimer's disease; aMCI, amnestic mild cognitive impairment; APOE ε4, apolipoprotein E ε4; DLB, dementia with Lewy bodies; FU, follow-up; GDepS, Geriatric Depression Scale; Min, minimal atrophy; MMSE, Mini–Mental State Examination; MT, medial temporal atrophy; NCs, normal controls; NPH, normal pressure hydrocephalus; PSPS, progressive supranuclear palsy syndrome; PT, parietotemporal atrophy; svPPA, semantic variant primary progressive aphasia; VaD, vascular dementia; WMH, white matter hyperintensity.

[a] Mild WMH, deep WMH <10 mm and periventricular WMH <5 mm; and Moderate WMH, deep WMH ≥10 mm or periventricular WMH ≥5 mm (patients with severe WMH defined as deep WMH ≥25 mm and periventricular WMH ≥10 mm were initially excluded).

Table 2
Hazard ratios of dementia conversion according to anatomical subtype

Variables	Model 1		Model 2		Model 3	
	HR (95% CI)	*p*	HR (95% CI)	*p*	HR (95% CI)	*p*
Anatomical subtype						
Minimal subtype	REF		REF		REF	
Medial temporal subtype	1.08 (0.74–1.59)	0.695	1.10 (0.75–1.61)	0.630	1.08 (0.74–1.59)	0.687
Parietotemporal subtype	1.51 (1.06–2.15)	0.024	1.47 (1.03–2.10)	0.033	1.45 (1.01–2.07)	0.042
Age			1.02 (1.00–1.04)	0.043	1.02 (1.00–1.04)	0.041
Education					1.02 (0.99–1.05)	0.100

Model 1: Anatomical subtype was entered as a predictor. Model 2: Age was entered as a predictor in addition to Model 1. Model 3: Education was entered as a predictor in addition to Model 2.
Key: CI, confidence interval; HR, hazard ratio.

imagingpattern) using 80 region of interests (ROIs) (Dong et al., 2016a,b), whereas we applied surface-based morphometry, which is more sensitive for detecting cortical atrophy, and we used approximately 80,000 vertices, an approach more suitable for high-dimensional data (Park et al., 2017). Third, our clustering method can be easily applied in clinical practice because it is based only on cortical thickness, which can be acquired through brain MRI and does not require incorporation of other biomarkers such as CSF amyloid/tau or molecular PET imaging (Nettiksimmons et al., 2014). Finally, none of the previous methods proposed an individual-level classification. Our classifier achieved a high accuracy of 89.6%, and we believe our method might serve as a useful means to predict the subtype and prognosis of individual aMCI patients.

Patients with the Min subtype did not show significant atrophy compared with NCs, had a relatively stable clinical course, and had the lowest frequency of amyloid PET positivity and APOE ε4 carriers, suggesting that non-neurodegenerative etiologies might underlie their cognitive impairment. We expected that the Min subtype might represent a more psychiatric form of MCI such as cognitive impairment associated with depression or vascular form of MCI, which results in lower cognitive function without neurodegeneration. However, the Min subtype did not show significant difference in scores on the Geriatric Depression Scale or in severity of WMHs compared with other subtypes. Therefore, we cannot completely exclude the possibility that patients with the Min subtype are in the very early stages of the AD process in which amyloid cannot be detected on PET scan. Alternatively, these patients might have some non-neurodegeneration causes that can contribute to cognitive impairment, which have not yet been identified.

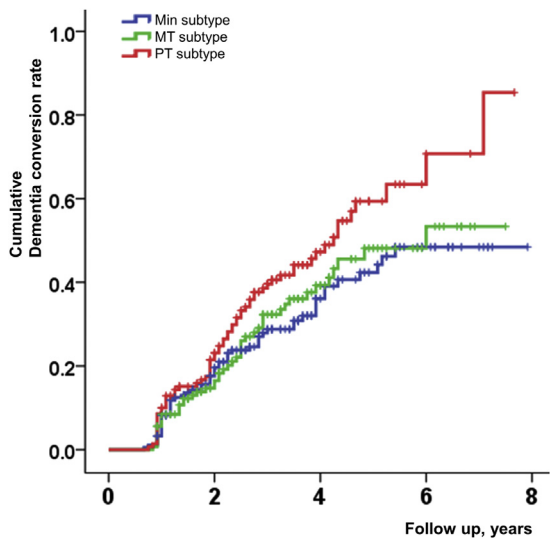

Fig. 3. Cumulative dementia conversion rate according to anatomical subtype of aMCI. Time 0 indicates the time when the diagnosis was made based on neuropsychological testing and brain MRI, which were performed with a median interval of 0 months (interquartile range 0-0). aMCI, amnestic mild cognitive impairment; MRI, magnetic resonance imaging; MT, medial temporal atrophy; Min, minimal atrophy; PT, parietotemporal atrophy.

In contrast, the PT subtype with a typical AD-like atrophy pattern proved to be a malignant type of aMCI. These patients had the highest frequency of amyloid PET positivity, APOE ε4 carriers, and showed the highest dementia conversion rate. This result is in line with previous studies showing that, among patients with AD dementia, those with parietal-dominant atrophy showed rapid cognitive decline (Na et al., 2016). A previous study that clustered anatomical subtypes of aMCI and AD dementia together showed similar results in that the subtype with PT showed classical AD characteristics with the fastest clinical progression (Dong et al., 2016b). Interestingly, our patients with PT subtype were not significantly different in age from the other subtypes. Previous studies on anatomical or pathological AD dementia subtypes showed that patients with parietal-dominant atrophy exhibited younger symptom-onset age (Noh et al., 2014). Our results suggest that, in patients with aMCI, PT predicts worse prognosis regardless of age.

Our third type of aMCI, the MT subtype, consisted of individuals with localized atrophy in the medial temporal areas. This subtype is consistently reported in most aMCI cluster studies (Dong et al., 2016b; Nettiksimmons et al., 2014), even in AD dementia (Murray et al., 2011; Noh et al., 2014) or subjective memory impairment (Jung et al., 2016) cluster studies, and has been referred to as "limbic-predominant" (Murray et al., 2011) or "medial-temporal-dominant" atrophy (Noh et al., 2014). Previous studies of AD dementia consistently showed that patients with focal medial temporal lobe dysfunction have a relatively slow rate of progression (Butters et al., 1996; Na et al., 2016). Thus, one possibility is that MT subtype might represent the earliest stage of this process. The underlying pathology of our patients with MT subtype might be AD (Murray et al., 2011). However, we also suspect that these patients might have hippocampal sclerosis or primary age-related tauopathy (Jellinger et al., 2015; Landau et al., 2016).

Although aMCI could be classified into distinct anatomical subtypes, we could not find differences in demographics or neuropsychological test results across the anatomical subtypes of aMCI. Cognitive scores might not capture regional differences in atrophy patterns and may lack the ability to detect heterogeneous atrophy patterns. Our results therefore suggest that anatomical classification can provide a more sensitive approach for defining aMCI subtypes. Furthermore, although APOE genotype, amyloid PET, or CSF level of amyloid and tau may predict prognosis of patients with aMCI, our classification algorithm may be more widely used because it only requires MRI data. These findings further emphasize the potential value of clustering patients based on brain atrophy patterns.

To the best of our knowledge, this is the first study to identify the anatomical subtypes of aMCI on an individual basis. The proposed method showed high accuracy for classification of aMCI subtypes (89.6%), which suggests that individual-level classification of aMCI subtypes based on distinct topographic patterns of cortical atrophy can be achieved by a simple but powerful method using LDA and PCA. More specifically, our binary classification models performed very well for distinguishing the PT subtype versus other subtypes (92.6%). This suggests that PT subtype has a unique characteristic atrophy pattern.

Our individual-level classifier has several advantages. First, it is an efficient method of analysis in the context of data accumulation. Previously, whenever researchers investigated the characteristics of each aMCI subtype, it was inevitable to perform a de novo cluster analysis at a group level. This is a crucial drawback in accumulating knowledge of each subtype, as we cannot guarantee whether the newly discovered aMCI subtypes are indeed identical to previously determined subtypes. As cluster analyses are based on similarities among individuals, the subtype results tend to be affected by the characteristics of a given aMCI population. Therefore, all cluster analyses require verification, which is time-consuming and inefficient. In this regard, a classifier that classifies aMCI into previously proven predetermined subtypes is needed. This allows researchers to focus on investigating the clinical findings of each subtype rather than on the validating aMCI patient clustering. Second, our individual-level classifier can be used in designing future clinical trials as it provides information about which subtype a new individual is likely to belong to. Our classifier can be applied to individual patients in clinical practice with relatively high accuracy and can be used as a biomarker to assist in the selection of patients who can benefit from upcoming AD disease-modifying therapies.

We acknowledge the limitations of this study. First, because we retrospectively collected data, the follow-up duration varied. However, there were no differences in follow-up duration across anatomical subtypes. Second, the sample was derived from a memory clinic, which may limit the accuracy of subtype classification in a more heterogeneous sample with greater vascular burden. Third, as the 3 subtypes might reflect different stages of the disease, further studies with longer follow-up duration are necessary. Finally, only a small number of patients underwent amyloid PET, and our data lacked tau biomarkers to confirm the underlying pathology.

Disclosure

The authors have no disclosures relevant to the manuscript to report.

Acknowledgements

This research was supported by a National Research Foundation of Korea grant funded by the Korean government (MSIP) (NRF-2018R1A1A3A04079255 and NRF-2017R1A2B2005081); the Korea Health Technology R&D Project, Ministry of Health and Welfare, Republic of Korea (HI14C2746, HI18C0335, and HI18C1629); and the Bio & Medical Technology Development Program of the NRF funded by Korean government, MSIP (2015M3A9A7029740) and Ministry of Science, ICT, & Future Planning (NRF-2016M3A9A7916996); and the Original Technology Research Program for Brain Science through the NRF of Korea funded by the Ministry of Science ICT and Future Planning (2017M3C7A1048566).

Authors' contributions: Design or conceptualization of the study was done by HJK, J-KS, and DLN. Analysis or interpretation of the data was done by J-YP, SWS, YHJ, YK, HJ, and STK. Drafting or revising the manuscript for intellectual content was done by HJK, J-KS, and DLN.

Appendix A. Supplementary data

Supplementary data to this article can be found online at https://doi.org/10.1016/j.neurobiolaging.2018.10.010.

References

Ahn, H.J., Chin, J., Park, A., Lee, B.H., Suh, M.K., Seo, S.W., Na, D.L., 2010. Seoul Neuropsychological Screening Battery-dementia version (SNSB-D): a useful tool for assessing and monitoring cognitive impairments in dementia patients. J. Korean Med. Sci. 25, 1071–1076.

American Psychiatric Association, 2000. Diagnostic and Statistical Manual of Mental Disorders, 4th ed., Text Revision. American Psychiatric Association, Washington, DC.

Barthel, H., Gertz, H.J., Dresel, S., Peters, O., Bartenstein, P., Buerger, K., Hiemeyer, F., Wittemer-Rump, S.M., Seibyl, J., Reininger, C., Sabri, O., Florbetaben Study, G., 2011. Cerebral amyloid-beta PET with florbetaben (18F) in patients with Alzheimer's disease and healthy controls: a multicentre phase 2 diagnostic study. Lancet Neurol. 10, 424–435.

Butters, M.A., Lopez, O.L., Becker, J.T., 1996. Focal temporal lobe dysfunction in probable Alzheimer's disease predicts a slow rate of cognitive decline. Neurology 46, 687–692.

Cho, Y., Seong, J.K., Jeong, Y., Shin, S.Y., Neuroimaging, A.D., 2012. Individual subject classification for Alzheimer's disease based on incremental learning using a spatial frequency representation of cortical thickness data. Neuroimage 59, 2217–2230.

Choi, S.H., Na, D.L., Lee, B.H., Hahm, D.S., Jeong, J.H., Jeong, Y., Koo, E.J., Ha, C.K., Ahn, S.S., 2002. The validity of the Korean version of global deterioration scale. J. Korean Neurol. Assoc. 20, 612–617.

Dale, A.M., Fischl, B., Sereno, M.I., 1999. Cortical surface-based analysis. I. Segmentation and surface reconstruction. Neuroimage 9, 179–194.

Dale, A.M., Sereno, M.I., 1993. Improved localizadon of cortical activity by combining EEG and MEG with MRI cortical surface reconstruction: a linear approach. J. Cogn. Neurosci. 5, 162–176.

Dong, A., Honnorat, N., Gaonkar, B., Davatzikos, C., 2016a. CHIMERA: clustering of heterogeneous disease effects via distribution matching of imaging patterns. IEEE Trans. Med. Imaging 35, 612–621.

Dong, A., Toledo, J.B., Honnorat, N., Doshi, J., Varol, E., Sotiras, A., Wolk, D., Trojanowski, J.Q., Davatzikos, C., Alzheimer's Disease Neuroimaging Initiative, 2016b. Heterogeneity of neuroanatomical patterns in prodromal Alzheimer's disease: links to cognition, progression and biomarkers. Brain 140, 735–747.

Groth, D., Hartmann, S., Klie, S., Selbig, J., 2013. Principal components analysis. Methods Mol. Biol. (Clifton, N.J.) 930, 527–547.

Jellinger, K.A., Alafuzoff, I., Attems, J., Beach, T.G., Cairns, N.J., Crary, J.F., Dickson, D.W., Hof, P.R., Hyman, B.T., Jack Jr., C.R., Jicha, G.A., Knopman, D.S., Kovacs, G.G., Mackenzie, I.R., Masliah, E., Montine, T.J., Nelson, P.T., Schmitt, F., Schneider, J.A., Serrano-Pozo, A., Thal, D.R., Toledo, J.B., Trojanowski, J.Q., Troncoso, J.C., Vonsattel, J.P., Wisniewski, T., 2015. PART, a distinct tauopathy, different from classical sporadic Alzheimer disease. Acta neuropathologica 129, 757–762.

Jung, N.Y., Seo, S.W., Yoo, H., Yang, J.J., Park, S., Kim, Y.J., Lee, J., Lee, J.S., Jang, Y.K., Lee, J.M., Kim, S.T., Kim, S., Kim, E.J., Na, D.L., Kim, H.J., 2016. Classifying anatomical subtypes of subjective memory impairment. Neurobiol. Aging 48, 53–60.

Kang, Y., Na, D.L., 2003. Seoul Neuropsychological Screening Battery (SNSB). Human Brain Research & Consulting, Incheon.

Knopman, D.S., Beiser, A., Machulda, M.M., Fields, J., Roberts, R.O., Pankratz, V.S., Aakre, J., Cha, R.H., Rocca, W.A., Mielke, M.M., Boeve, B.F., Devine, S., Ivnik, R.J., Au, R., Auerbach, S., Wolf, P.A., Seshadri, S., Petersen, R.C., 2015. Spectrum of cognition short of dementia Framingham heart study and Mayo clinic study of aging. Neurology 85, 1712–1721.

Ku, H.M., K, J., Kwon, E.J., Kim, S.H., Lee, H.S., Ko, H.J., Jo, S., Kim, D.K., 2004. A study on the reliability and validity of Seoul-instrumental activities of daily living (S-IADL). J. Korean Neuropsychiatr. Assoc. 43, 189–199.

Landau, S.M., Horng, A., Fero, A., Jagust, W.J., Alzheimer's Disease Neuroimaging, I., 2016. Amyloid negativity in patients with clinically diagnosed Alzheimer disease and MCI. Neurology 86, 1377–1385.

Lee, J.H., Kim, S.H., Kim, G.H., Seo, S.W., Park, H.K., Oh, S.J., Kim, J.S., Cheong, H.K., Na, D.L., 2011. Identification of pure subcortical vascular dementia using 11C-Pittsburgh compound B. Neurology 77, 18–25.

Liu, C., Wechsler, H., 2000. Robust coding schemes for indexing and retrieval from large face databases. IEEE Trans. Image Process. 9, 132–137.

McGuinness, B., Barrett, S.L., McIlvenna, J., Passmore, A.P., Shorter, G.W., 2015. Predicting conversion to dementia in a memory clinic: a standard clinical approach compared with an empirically defined clustering method (latent profile analysis) for mild cognitive impairment subtyping. Alzheimers Dement (Amst) 1, 447–454.

Murray, M.E., Graff-Radford, N.R., Ross, O.A., Petersen, R.C., Duara, R., Dickson, D.W., 2011. Neuropathologically defined subtypes of Alzheimer's disease with distinct clinical characteristics: a retrospective study. Lancet Neurol. 10, 785–796.

Na, H.K., Kang, D.R., Kim, S., Seo, S.W., Heilman, K.M., Noh, Y., Na, D.L., 2016. Malignant progression in parietal-dominant atrophy subtype of Alzheimer's disease occurs independent of onset age. Neurobiol. Aging 47, 149–156.

Nettiksimmons, J., DeCarli, C., Landau, S., Beckett, L., Alzheimer's Disease Neuroimaging, I., 2014. Biological heterogeneity in ADNI amnestic mild cognitive impairment. Alzheimers Dement 10, 511–521 e511.

Noh, Y., Jeon, S., Lee, J.M., Seo, S.W., Kim, G.H., Cho, H., Ye, B.S., Yoon, C.W., Kim, H.J., Chin, J., Park, K.H., Heilman, K.M., Na, D.L., 2014. Anatomical heterogeneity of Alzheimer disease: based on cortical thickness on MRIs. Neurology 83, 1936–1944.

Ota, K., Oishi, N., Ito, K., Fukuyama, H., Group, S.-J.S., Alzheimer's Disease Neuroimaging, I., 2016. Prediction of Alzheimer's disease in amnestic mild cognitive impairment subtypes: stratification based on imaging biomarkers. J. Alzheimers Dis. 52, 1385–1401.

Park, J.Y., Na, H.K., Kim, S., Kim, H., Kim, H.J., Seo, S.W., Na, D.L., Han, C.E., Seong, J.K., Alzheimer's Disease Neuroimaging, I., 2017. Robust Identification of Alzheimer's Disease subtypes based on cortical atrophy patterns. Sci. Rep. 7, 43270.

Petersen, R.C., 2004. Mild cognitive impairment as a diagnostic entity. J. Intern. Med. 256, 183–194.

Petersen, R.C., Smith, G.E., Waring, S.C., Ivnik, R.J., Tangalos, E.G., Kokmen, E., 1999. Mild cognitive impairment: clinical characterization and outcome. Arch. Neurol. 56, 303–308.

Pusswald, G., Moser, D., Gleiss, A., Janzek-Hawlat, S., Auff, E., Dal-Bianco, P., Lehrner, J., 2013. Prevalence of mild cognitive impairment subtypes in patients attending a memory outpatient clinic–comparison of two modes of mild cognitive impairment classification. Results of the Vienna Conversion to Dementia Study. Alzheimers Dement 9, 366–376.

Qiu, A.Q., Bitouk, D., Miller, M.I., 2006. Smooth functional and structural maps on the neocortex via orthonormal bases of the Laplace-Beltrami operator. Ieee T Med. Imaging 25, 1296–1306.

Shim, Y.S., Morris, J.C., 2011. Biomarkers predicting Alzheimer's disease in cognitively normal aging. J. Clin. Neurol. (Seoul, Korea) 7, 60–68.

Vos, S.J.B., Verhey, F., Frolich, L., Kornhuber, J., Wiltfang, J., Maier, W., Peters, O., Ruther, E., Nobili, F., Morbelli, S., Frisoni, G.B., Drzezga, A., Didic, M., van Berckel, B.N.M., Simmons, A., Soininen, H., Kloszewska, I., Mecocci, P., Tsolaki, M., Vellas, B., Lovestone, S., Muscio, C., Herukka, S.K., Salmon, E., Bastin, C., Wallin, A., Nordlund, A., de Mendonca, A., Silva, D., Santana, I., Lemos, R., Engelborghs, S., Van der Mussele, S., Freund-Levi, Y., Wallin, A.K., Hampel, H., van der Flier, W., Scheltens, P., Visser, P.J., Initi, A.s.D.N., 2015. Prevalence and prognosis of Alzheimer's disease at the mild cognitive impairment stage. Brain 138, 1327–1338.

Yu, H., Yang, H., 2001. A direct LDA algorithm for high-dimensional data - with application to face recognition. Pattern Recogn 34, 2067–2070.

Zhang, N., Song, X., Zhang, Y., Alzheimer's Disease Neuroimaging, I., 2012. Combining structural brain changes improves the prediction of Alzheimer's disease and mild cognitive impairment. Dement Geriatr. Cogn. Disord. 33, 318–326.